Results in Physics 55 (2023) 107155

Contents lists available at ScienceDirect

Results in Physics

journal homepage: www.elsevier.com/locate/rinp

Wigner quasi-probability distribution of a resonator coherent field interacting with a flux qubit via two-photon coupling

Laila A. Al-essa [a,1], Wafa F. Alfwzan [a,1], F.M. Aldosari [b,1], A.-B.A. Mohamed [b,1,*], H. Eleuch [c,d,e,1]

[a] Department of Mathematical Sciences, College of Science, Princess Nourah bint Abdulrahman University, P.O. Box 84428, Riyadh 11671, Saudi Arabia
[b] Department of Mathematics, College of Science and Humanities in Al-Aflaj, Prince Sattam bin Abdulaziz University, Saudi Arabia
[c] Department of Applied Physics and Astronomy, University of Sharjah, Sharjah, United Arab Emirates
[d] College of Arts and Sciences, Abu Dhabi University, Abu Dhabi 59911, United Arab Emirates
[e] Institute for Quantum Science and Engineering, Texas A&M University, College Station, TX 77843, USA

ARTICLE INFO

Keywords:
Wigner-distribution
Flux-qubit
Resonator coherent field

ABSTRACT

The Wigner quasi-probability distribution function is an important tool for estimating the quantumness of quantum states. The Wigner distribution function (WDF) is related monotonically to the coherent field state density operator and their probability distributions. In this paper, we analyze the time-dependent resonator coherent field states produced by a flux qubit's interaction with a resonator-field through a two-photon coupling. The WDF dynamics of the coherent field states is investigated under the effects of the qubit-resonator detuning and the intrinsic decoherence. The WDF non-classicality associated with the mixedness resonator entropy dynamics can be controlled by varying the qubit-resonator interaction, detuning as well as the decoherence. The intrinsic decoherence clearly affects the WDF non-classicality, identified by the negative values of the WDF. Finally, by fixing one or both of the complex phase space components, we are able to explore the dynamics of the Wigner-distribution functions.

Introduction

It has previously been shown that quasi-probability distribution functions such as Husimi and Wigner functions [1,2], are crucial tools for analyzing quantum phase-space information resources, such as non-classicality, mixedness, and entanglement [3,4]. Here, we quantify the positivity and negativity of the Wigner quasi-probabilities, which are related with the classicality and non-classicality of a quantum system [5–7]. Nonclassical features (as non-Gaussanity, non-classicality, and Robustness of Wigner function negativity) have been explored in different real systems, such as spin-qubit systems [8], nonlinear optical medium cavity, and quantum well system [9], exciton-exciton interactions inside two coupled semiconductor quantum dots [10], and photon-added coherent states [11]. Based on the negativity of the non-Gaussanity of a multimode light field has been reconstructed, experimentally [12]. The non-classicality of the Wigner function has been investigated under the effect of intrinsic decoherence [13]. The Wigner function has been applied to quantify the non-classical properties of a f-deformed system [14], and a resonator-qubit [15]. The superposed-coherent-states non-classicality has an effective role to enhance quantum effects [16–18]. The superposed coherent states has been realized in superconducting junction [19,20] and optical systems [21].

Several physical systems have been proposed to implement qubits, including quantum dots [22], magnons coupled to an open microwave cavity [23,24], trapped ions [25], nitrogen-vacancy centers located in crystal cavities [26,27], and superconducting circuits [28–31]. Superconducting circuits' artificial qubits have high flexibility to implement qubit interacting with resonators through multi-photon transitions [32,33]. Qubit-resonator interactions have been used to realized various nonlinear-optics phenomena [34,35]. Qubit-resonator interactions with single-photon process has been proposed by using junction-flux-qubit superconducting circuits [15,36,37]. After that, superconducting circuits have been proposed to implement a two-photon qubi-resonator interaction quantum Rabi model [38]. The realization of nonlinear two-photon qubit-photon interactions in [39] pave the way for various investigations on the quantum effects in superconducting circuits' artificial qubits with nonlinear interactions. Recently, it has been shown that the quantum memory-assisted entropic uncertainty relation and the non-Markovian dynamics of two-qubit entanglement two two-level atoms can be enhanced and protected when the two qubits are coupled to a cavity with two-photon relaxation [40,41].

* Corresponding author.
E-mail address: abdelbastm@aun.edu.eg (A.-B. Mohamed).
[1] Contributed equally to the manuscript.

https://doi.org/10.1016/j.rinp.2023.107155
Received 19 July 2023; Received in revised form 28 October 2023; Accepted 1 November 2023
Available online 3 November 2023

The features of a quantum state, especially non-classicality, are very sensitive to decoherence and dissipation [42–44], the intrinsic decoherence will be here considered to explore the and Wigner-distribution non-classicality dynamics. For closed quantum system, in our case a qubit interacting with the cavity, Milburn equation [44] is utilized to study the dynamics of quantum information resources. While for open quantum systems, the master equations [45,46], are used to investigate the dissipation and decoherence effects. The Milburn intrinsic decoherence equation is used to analyze the decoherence effect in various quantum systems [47–50], such as trapped-ion systems and superconducting systems [51,52].

Interactions of qubits with nonclassical coherent field states have significant roles on the nonclassical effects [53,54]. So, the field-states non-classicality needs to be investigated further for the quantum information resources. In the context of the two-photon interaction and the decoherence effect, we investigate the generated resonator-field-state Wigner non-classicality produced by interactions of a SC flux qubit with an even coherent resonator coherent field (that has a high initial non-classicality).

The second section that follows describes the qubit-resonator dynamics affected by the intrinsic decoherence. The third part provides illustrations of the Wigner phase space non-classicality dynamics. The fourth section presents our conclusions.

Qubit-resonator dynamics induced by decoherence model

To explore the temporal qubit-resonator density matrix dynamics under the intrinsic decoherence, we use the Milburn intrinsic equation [44],

$$\begin{aligned} \frac{d\hat{M}_{QR}(t)}{dt} &= \hat{L}\hat{M}_{QR}, \\ \hat{L}\hat{M}_{QR} &= -i[\hat{H}_{QR}, \hat{M}_{QR}] - \frac{\gamma}{2}[\hat{H}_{QR}, [\hat{H}_{QR}, \hat{M}_{QR}]], \end{aligned} \tag{1}$$

where $\hat{M}_{QR}(t)$ represents the density matrix. γ is the decoherence rate. The qubit-resonator Hamiltonian $\hat{H}_{QR}$ describes two junctions coupled to a superconducting(SC)-flux qubit [31,38] to engineering a qubit-resonator interaction through two-photon transitions. The superconducting circuit of the two-photon qubit-resonator interactions consisting of two identical junctions inductively coupled to a superconducting-flux qubit. For the quadratic coupling, the qubit-resonator Hamiltonian is given by ($\hbar = 1$) [38]

$$\hat{H}_{QR} = \omega_R(\hat{a}_R^{\dagger}\hat{a}_R + \frac{1}{2}) + \frac{1}{2}\omega_Q\hat{\sigma}_Q^z + \lambda(\hat{a}_R + \hat{a}_R^{\dagger})^2\hat{\sigma}_Q^x. \tag{2}$$

The resonator-mode field has a transition frequency ω_R and the annihilation operator of the resonator field is identified by $\hat{a}_R$. While the flux qubit is described by: the frequency ω_Q, inversion operator $\hat{\sigma}_Q^z$, $\hat{\sigma}_Q^x$, and the annihilation Pauli operator $|0_Q\rangle\langle 1_Q|$ with the lower $|0_Q\rangle$ and upper $|1_Q\rangle$ energy levels. The qubit-resonator coupling is given by

$$\lambda = -\frac{\pi}{4}\tan(\frac{\pi\Phi_E}{\Phi_0})\frac{DI}{\Phi_0}\omega_R, \tag{3}$$

where flux qubits described by: the mutual flux qubit inductance D, the current I as well as the quantum Φ_0 and the external static Φ_E fluxes. Here, we consider the SC regime [31], in which the qubit-resonator coupling is smaller than the qubit and cavity eigenfrequencies, and it is greater than the dissipation rates. The counter-rotating terms: $(|0_Q\rangle\langle 1_Q|\hat{a}^2 + H.c.)$ and $(\hat{\sigma}_x\hat{a}^{\dagger}\hat{a})$ can then be neglected. Therefore, the Hamiltonian is given by [38]

$$\begin{aligned} \hat{H}_{QR} &= \omega_R(\hat{a}_R^{\dagger}\hat{a}_R + \hat{\sigma}_Q^z) + \frac{\delta}{2}\hat{\sigma}_Q^z \\ &\quad + \lambda(\hat{a}_R^2|1_Q\rangle\langle 0_Q| + |0_Q\rangle\langle 1_Q|\hat{a}_R^{2\dagger}). \end{aligned} \tag{4}$$

The difference between frequencies of the qubit and the resonator-field is represented by the detuning, $\delta = \omega_Q - 2\omega_R$.

By using the qubit-resonator basis: $\{|S_1\rangle = |1, n\rangle, |S_2\rangle = |0, n+2\rangle\}(n = 0, 1, 2, \ldots)$, the qubit-resonator Hamiltonian eigenstates have the following expression:

$$\begin{aligned} |V_1^n\rangle &= F_n|S_1\rangle + G_n|S_2\rangle, \\ |V_2^n\rangle &= G_n|S_1\rangle - F_n|S_2\rangle, \end{aligned} \tag{5}$$

where

$$\begin{aligned} F_n &= \sqrt{(R_n + \delta)/2R_n}, \qquad G_n = \sqrt{(R_n - \delta)/2R_n}, \\ R_n &= \sqrt{\delta^2 + \lambda^2(n+1)(n+2)}. \end{aligned} \tag{6}$$

The qubit-resonator Hamiltonian eigenvalues are:

$$\begin{aligned} V_1^n &= \omega_R(n+2) + \lambda\sqrt{[(\omega_Q - 2\omega_R)/\lambda]^2 + n^2 + 3n + 2}, \\ V_2^n &= \omega_R(n+2) - \lambda\sqrt{[(\omega_Q - 2\omega_R)/\lambda]^2 + n^2 + 3n + 2}. \end{aligned}$$

To find an analytical description for the Milburn intrinsic decoherence equation (1), we consider the initial qubit-resonator density matrix $M(0)$ described by a flux qubit upper state $|1_Q\rangle\langle 1_Q|$ coupled to an even resonator coherent-field state $(|\beta\rangle + |-\beta\rangle)/2$ that has the following photon distribution,

$$D_n = \frac{[1 + (-1)^n]\beta^n e^{-\frac{1}{2}|\beta|^2}}{2(1 + \langle\beta| - \beta\rangle)\sqrt{n!}}. \tag{7}$$

We focus on the case where the initial state is an even coherent state. The non-classicality of the coherent-field state can be identified by the negative values of the phase space Wigner distribution function.

By using Eq. (1) with the initial qubit-resonator state $\hat{M}(0)$, the generated time-dependent qubit-resonator state is given by [55]

$$\hat{M}_{QR}(t) = \sum_{m,n=0}\sum_{i,j=1,2} X_{ij}^{mn} H_{ij}^{mn}|V_i^m\rangle\langle V_j^n|, \tag{8}$$

with

$$X_{ij}^{mn} = e^{-i(V_i^m - V_j^n)t} I_D, \quad H_{ij}^{mn} = \langle V_i^m|\hat{M}(0)|V_j^n\rangle.$$

The decoherence term is: $I_D = e^{-\frac{\gamma}{2}(V_k^m - V_l^n)^2 t}$.

Now, based on the initial state, the qubit-resonator state dynamics has the following expression:

$$\begin{aligned} \hat{M}_{QR}(t) = \sum_{m,n=0} & D_m D_n^*[F_m F_n E_{11}|V_1^m\rangle\langle V_1^n| + F_m G_n \\ & \times E_{12}|V_1^m\rangle\langle V_2^n| + G_m F_n E_{21}|V_2^m\rangle\langle V_1^n| \\ & + G_m G_n E_{22}|V_2^m\rangle\langle V_2^n|], \end{aligned} \tag{9}$$

The coefficients E_{ij} are given by

$$\begin{aligned} E_{11} &= X_{11}^{mn} + X_{mn}^{12} + X_{21}^{mn} + X_{22}^{mn}, \\ E_{12} &= X_{11}^{mn} - X_{mn}^{12} + X_{21}^{mn} - X_{22}^{mn}, \\ E_{21} &= X_{11}^{mn} + X_{mn}^{12} - X_{21}^{mn} - X_{22}^{mn}, \\ E_{22} &= X_{11}^{mn} - X_{mn}^{12} - X_{21}^{mn} + X_{22}^{mn}. \end{aligned} \tag{10}$$

The reduced resonator-field density matrix needed for the analysis of the Wigner distribution function can be expressed as following:

$$\hat{M}^R(t) = \sum_{m,n=0} D_m D_n^* (A_{mn}^R(t)|m\rangle\langle n| + B_{mn}^R(t)|m+2\rangle\langle n+2|), \tag{11}$$

with

$$A_{mn}^R(t) = F_m^2 F_n^2 X_{11}^{mn} + F_m^2 G_n^2 X_{12}^{mn} + G_m^2 F_n^2 X_{2l}^{mn} + G_m^2 G_n^2 X_{22}^{mn},$$
$$B_{mn}^R(t) = F_m F_n G_m G_n (X_{11}^{mn} - X_{12}^{mn} - X_{21}^{mn} + X_{22}^{mn}).$$

Wigner distribution function (WDF)

For the considered subsystem resonator field with the reduced density matrix $\hat{M}^R(t)$, the symmetric Wigner characteristic function [56] is given by

$$C_\mu^W = Tr[\hat{M}^R(t)\hat{D}_\mu], \tag{12}$$

where $\hat{D}_\mu = \exp(\mu\hat{a}^+ - \mu^*\hat{a})$ is the displacement coherent-state field operator. The Wigner quasi-probability distribution is defined as

$$WD = \frac{1}{\pi^2}\int C_\mu^W \exp(\alpha\mu^* - \alpha^*\mu)d^2\mu. \tag{13}$$

This Wigner distribution function in the integral form is not always easy to calculate. To avoid the different calculation of the phase space integration, the WD integral form is expressed by using displaced number-state representation [57,58]. After writing the reduced resonator-field density $\hat{M}^R(t)$ of Eq. (11) in number-state representation as:

$$\hat{M}^R(t) = \sum_{m,n=0}^{\infty} A_{mn}^R(t)|m\rangle\langle n| + B_{mn}^R(t)|m+2\rangle\langle n+2|,$$

the expression of the time-dependent Wigner quasi-probability function is given by

$$W(\alpha,t) = \frac{2}{\pi}\sum_{k=0}^{\infty}\sum_{m,n=0}^{\infty}(-1)^k[A_{mn}^R(t)\Gamma_{k,n}(\alpha)\Gamma_{m,k}(\alpha) + B_{mn}^R(t)\Gamma_{k,n+2}(\alpha)\Gamma_{m+2,k}(\alpha)], \tag{14}$$

where

$$\Gamma_{k,n}(\alpha) = \exp(\frac{-|\alpha|^2}{2})\sum_{j=0}^{min(k,n)}\frac{(-\alpha)^{(k-j)}(\alpha^*)^{n-j}\sqrt{k!n!}}{(n-j)!(k-j)!j!}, \tag{15}$$

In the following section, we will examine the temporal Wigner quasi-probability function evolution in the presence of intrinsic decoherence.

Wigner distribution dynamics

Wigner phase space distribution non-classicality

Figs. 1(a-d) illustrate the dynamics of the Wigner distribution function (WDF) of the generated even-coherent-resonator state without the decoherence for the initial even-coherent-resonator intensity $\beta = 4$ at the resonance, $\delta = 0$. The even-coherent-resonator Wigner distribution is plotted for different times. The purpose of selecting the different specific times to investigate the even-coherent-resonator Wigner distribution dynamics for different generated coherent-resonator field states: the initial even-coherent-resonator pure state at $\lambda t = 0$ in (a), in a maximally coherent-resonator state at $\lambda t = 0.4425\pi$ in (b), and in a generated partial coherent-resonator mixed state at $\lambda t = \frac{3\pi}{4}$ in (c). If the coherent-resonator states are pure states as the initial even-coherent-resonator approximately, the WDF is plotted at $\lambda t = \pi$ in (d). The generated coherent-resonator field states due to the unitary interaction are shown in Fig. 1(e). The resonator entropy dynamics determines the selection of the various specific times. Without the intrinsic decoherence, the unitary qubit-resonator evolution has no effect on the coherence of the qubit-resonator, hence the entropy of the qubit-resonator vanishes. As a result, the Araki-Lieb inequality [59] states that the entropies of the qubit and resonator are equal. In this case, one of them is used to measure the qubit/resonator mixedness [60–62] that is the same as the qubit-resonator entanglement. By using the eigenvalues λ_n^R of the matrix of $\hat{M}^R(t)$, the resonator entropy dynamics is given by: $E_R(t) = -\sum_{n=1}\lambda_n^R \ln\lambda_n^R$. For the pure state, $E_R(t) = 0$. Otherwise for partially and maximally mixed states, $0 < E_R(t) \leq \ln 2$. At the resonance ($\delta = 0$), The resonator entropy $E_R(t)$ exhibits regular 2π-period oscillatory dynamics. The generated coherent-resonator field periodically exhibits a pure state (at $\lambda t = n\pi(n = 0, 1, 2, \ldots)$). The green dashed curve in Fig. 1(e) demonstrates that the periodicity of the resonator entropy vanishes for the off-resonance case ($\delta = 20\lambda$). Nonetheless the amplitudes of the entropy is enhanced, i.e., the qubit/resonator mixedness increases. The dash-dot curve shows the growth of the mixedness resonator entropy due to the increase of the intrinsic decoherence. The growth of entropy is linked to the influence of the intrinsic qubit-resonator decoherence term represented by: $I_D = e^{-\frac{\gamma}{2}(V_k^m - V_l^n)^2 t}$. This term contributes to the suppression of the off-diagonal elements of the density matrix, indicating the decay of quantum coherence. Consequently, this decay leads to an increase in entropy, reflecting the enhanced disorder or unpredictability within the quantum system. Understanding how such decoherence affects the dependability and predictability of quantum systems is critical in domains such as quantum computing and quantum information theory.

Fig. 1a illustrates the initial even-coherent-resonator Wigner distribution $W(\alpha, 0)$ (where $\alpha = x + iy$ where x, y are real) in the phase space for $x \in [-1.6\pi, 1.6\pi]$ and $y \in [0, 1.5\pi]$. The maxima and minima of the initial even-coherent-resonator Wigner function has symmetrical distribution with respect to $x-$ and $y-$ axes, which are clearly detectable in the phase space. The maxima and minima of the Wigner function are near the origin. The even-coherent-resonator states $|\beta\rangle$ and $|-\beta\rangle$ contribute to that the WDF shape which has two Poissonian photon number distributions (two separate peaks). While the quantum interference between the even-coherent-resonator states contributes to form interfered bottoms and peaks along the phase space y-axis. The maxima and minima of the interference bottoms and peaks are reduced and revive in the direction of increasing y-axis. The WDF negative values represent the non-classicality signature of the coherent-resonator field state.

Fig. 1b shows the WDF non-classicality $W(\alpha, 0.4425\pi)$ of the corresponding maximally mixed coherent-resonator state (when the corresponding resonator entropy is at maximum), which is generated due to unitary qubit-resonator interaction. The negativity and positivity of the symmetric interference fringes, compared to their initial values, are reduced and centered around the origin. While the WDF shapes of the initial two positive Gaussian peaks, induced by the coherent-resonator states $|\beta\rangle$ and $|-\beta\rangle$, are rotated by "90 degrees" to form a positive suppressed Gaussian peak at the end of the y-axis phase space.

When Fig. 1a results of the Wigner distribution $W(\alpha, 0)$ are compared with Fig. 1b results of the Wigner distribution $W(\alpha, 0.75\pi)$, we observe that the amplitudes of the negativity and positivity of the Wigner distribution of the initial pure coherent state (at $\lambda t = 0.4425\pi$) $W(\alpha, 0.4425\pi)$ increase, i.e. the non-classicality is enhanced to be very closed to that of a Wigner distribution for a superposition of the coherent-resonator states $|\beta\rangle$ and $|-\beta\rangle$. Figs. 1(d) show the WDFs $W(\alpha, \pi)$ of the corresponding pure coherent-resonator states (the resonator entropy $E_R(\pi) \simeq E_R(2\pi) \simeq 0.0$). If $W(\alpha, 2\pi)$ is plotted, we find that in this case the Wigner distribution closely resembles to $W(\alpha, 0)$. The non-classicalities of the two generated pure states are very similar to that of the initial pure state of Fig. 1a. This demonstrates that information on the non-classicality can be obtained from both the Wigner distribution and the resonator entropy.

From Figs. 2(a,b), we find that the non-classicalities of $W(\alpha, 0.75\pi)$ and $W(\alpha, 2\pi)$, are more affected by the detuning. The negativity and positivity of the generated symmetric interference fringes, compared to Figs. 2(b,f), are enhanced. While the regularity of the WDF shape

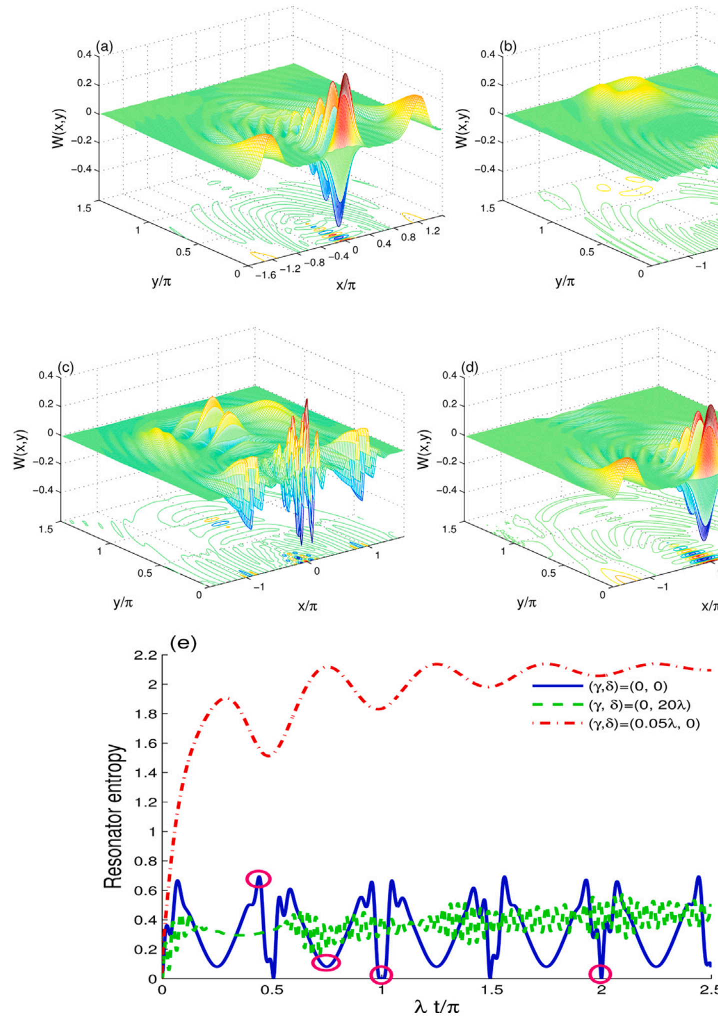

Fig. 1. WDF is depicted for $\beta = 4$, $\delta = 0$, and $\gamma = 0$ at different normalized times: $\lambda t = 0$ in (a), $\lambda t = 0.4425\pi$ in (b), $\lambda t = \frac{3\pi}{4}$ in (c), and $\lambda t = \pi$ in (d). In (e), the dynamic resonator entropy is plotted for different detuning and decoherence rates.

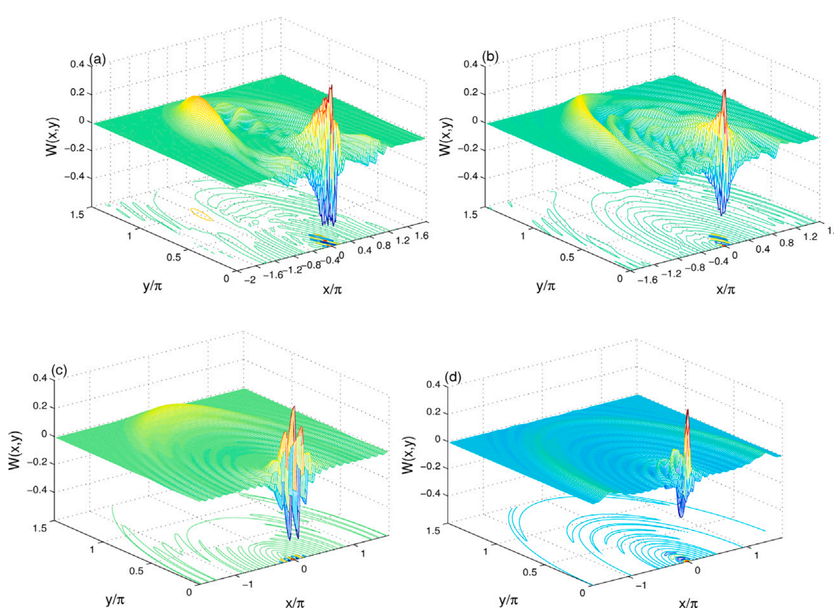

Fig. 2. WDFs of the corresponding the coherent-resonator states: $W(\alpha, 0.4425\pi)$ of Fig. 1b and $W(\alpha, 2\pi)$ of Fig. 1e, are depicted respectively under the qubit-resonator detuning effect ($\delta = 20\lambda$) in (a) and (b) and under the decoherence effect in (c) and (d), $\gamma = 0.05\lambda$.

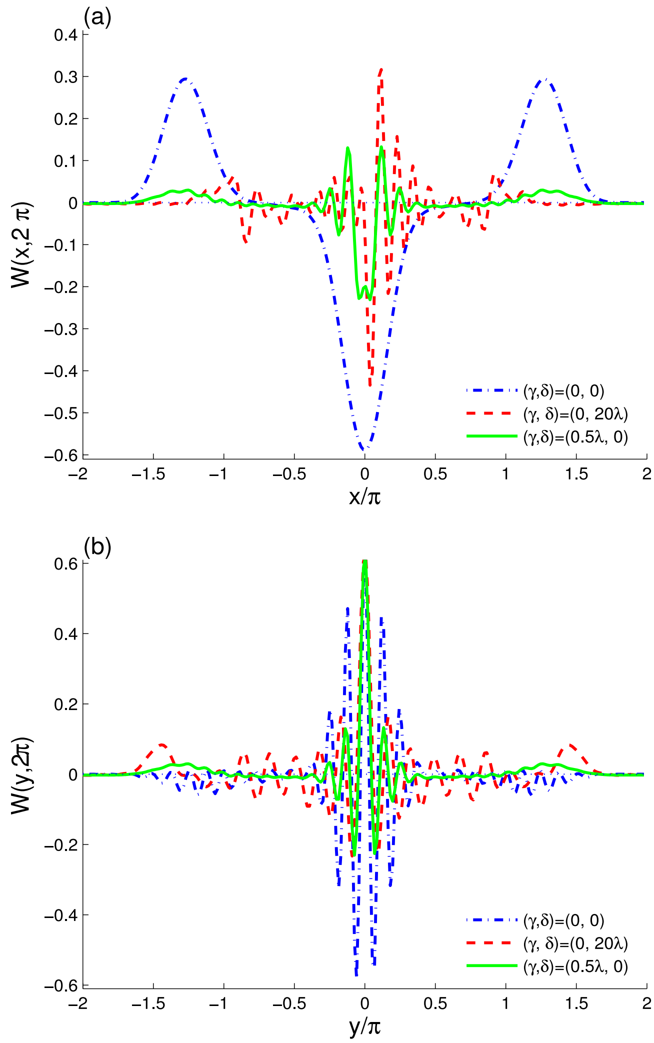

Fig. 3. The partial Wigner distributions $W(x, 2\pi)$ at $y = 0.063\pi$ and $W(y, 2\pi)$ at $x = 0$ are shown in (a) and (b) respectively for different detuning in the decoherence cases of (γ, δ).

of the two positive Gaussian peaks, corresponding to the two opposite the coherent-resonator states $|\beta\rangle$ and $|-\beta\rangle$, is disappeared. This means that the increased qubit-resonator detuning leads to generating another superposition of the coherent-resonator state that differs from the considered initial even coherent-resonator state. According to Fig. 2b, the non-classicality of the Wigner distribution function $W(\alpha, 0.75\pi)$ is more resistant to an increase in qubit-resonator detuning than the one linked to $W(\alpha, 2\pi)$ with the corresponding pure coherent-resonator state at $\lambda t = 2\pi$.

Figs. 2(c,d) illustrate the Wigner distribution non-classicality dynamics, for $W(\alpha, 0.4425\pi)$ and $W(\alpha, 2\pi)$, of the corresponding maximally mixed and pure coherent states with the decoherence, $\gamma = 0.5\lambda$. Because the associated maximally mixed coherent-resonator state is independent of the decoherence, the Wigner distribution non-classicality $W(\alpha, 0.4425\pi)$ of this state (whose resonator entropy is maximum) is very weak. The intrinsic decoherence totally erases the non-classicality information of the Wigner distribution $W(\alpha, 2\pi)$ with the exception of minor positive and negative peaks around the origin. According to Fig. 2b, the function $W(\alpha, 0.75\pi)$'s non-classicality is more resistant to qubit resonator decoherence than $W(\alpha, 2\pi)$ of the comparable 2π-pure coherent resonator state.

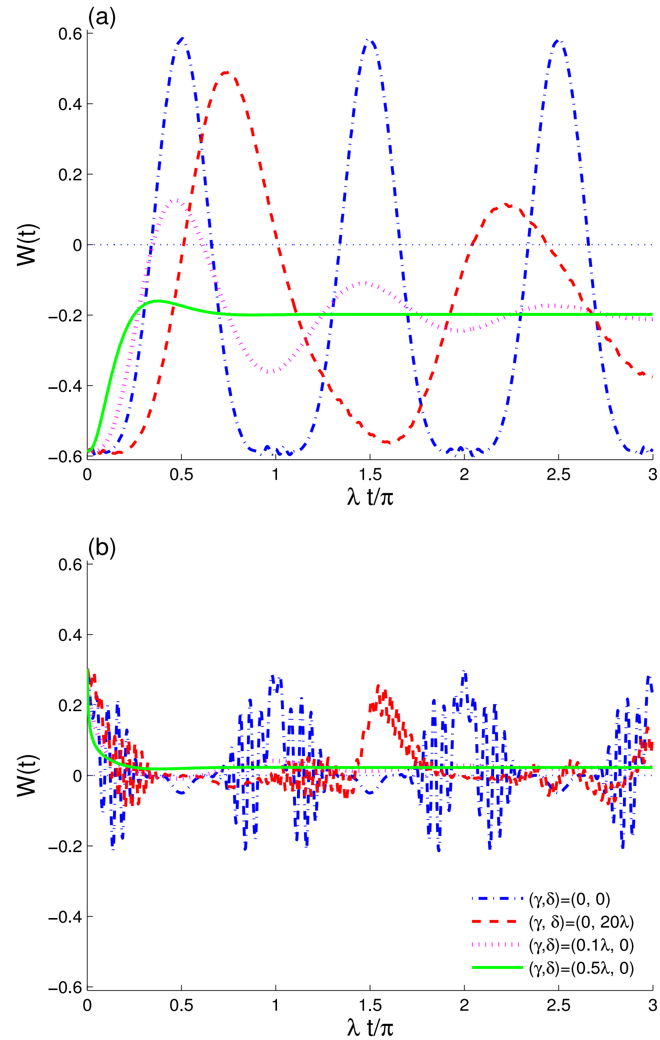

Fig. 4. The dynamics of the highest negativity and positivity's Wigner distribution are shown in (a) and (b) respectively under the effects of the qubit-resonator detuning in the decoherence for different cases of (γ, δ).

Partial WDF non-classicality dynamics

Here, we explore the dependence of the WDF non-classicality dynamics, on the real and imaginer component of the complex phase space. We analyze the qubit-resonator interaction, detuning, and decoherence effects. In Figs. 3(a,b), we study the impacts of the detuning and the decoherence on the dynamics of the partial Wigner distribution functions $W(x, 2\pi)$ at $y = 0.063\pi$ (see Fig. 3a), and $W(y, 2\pi)$ at $x = 0$ (see 3a). This is to analyze the maxima and minima WDF behaviors of $W(0 + i0.063\pi, 2\pi)$ of the corresponding generated pure coherent state at $\lambda t = 2\pi$. The dashed-dot curve in Fig. 3a shows that the vertical part of the Wigner distribution shape of Fig. 1e has two symmetric peaks and a minimum at $x = 0$. The WDF presents pronounced symmetric positivity (classicality) and negativity (non-classicality) behaviors as in Fig. 1e. By increasing the detuning or the decoherence, dashed and solid curves illustrate the amplitude reductions of the Wigner distribution $W(x, 2\pi)$. Therefore, the WDF non-classicality feature is weakened. The collapse and revival phenomena are noted. The qubit-resonator detuning leads to asymmetric WDF non-classicality behavior. Fig. 3b shows the dependence of the symmetric WDF positivity and negativity behavior on the phase space imaginer y-component. The appearance of the WDF oscillatory behavior around the origin, with large amplitudes and a high frequency, confirms the high sensitivity of the WDF non-classicality to the phase space imaginer y-component. The detuning and the intrinsic decoherence reduce the WD y-component oscillatory amplitudes. The maxima and minima interferences are enhanced and decreased by increasing the detuning and decoherence, respectively.

Fig. 4a illustrates the dynamics of the largest negative value of the Wigner distribution function $W(t) = W(i0.063\pi, t)$ (the time-partial Wigner distribution). From the dash-dot curve of Fig. 4a, we observe that the unitary qubit-resonator interaction leads to regular oscillatory behavior with π-period of the Wigner distribution, which fluctuates periodically between it extreme values ± 0.6, approximately. While the dashed curve of Fig. 4a shows that the time-partial Wigner distribution positivity is reduced by increasing the qubit-resonator detuning, $\delta = 20\lambda$, as time evolves The damped oscillatory dynamics are caused by increasing qubit-resonator detuning, which enhances the excitation of the cavity-field states. This leads to significant entanglement and nonclassical behavior. As a result, it confirms the strong ability of qubit-resonator detuning to magnify the non-classical properties of the Wigner distribution function (WDF), as highlighted in Refs. [63,64] and displayed in Fig. 1e. As time evolves, we find that the increase of the decoherence decreases the amplitude and frequency of the WD negativity dynamics, see Fig. 4a. For high decoherence and after a short time, the time-partial Wigner distribution reaches its stationary negativity this is time-independent, $W(t = \infty) \simeq -2$. The appearance of stationary WDF non-classicality behavior depends on the detuning and decoherence. Fig. 4b aims to explore the amount of the WDF non-classicality dynamics of a partial positive value of the corresponding $W(t) = W(-1.234\pi; +i0.03183\pi, t)$. Due to the unitary qubit-resonator interaction, the Wigner distribution non-classicality presents regular oscillatory behavior with π-period and also illustrates the collapse and revival phenomena. The dashed curve prove that the qubit-resonator detuning enhances the non-classicality of the WDF. While the dot and solid curves in Fig. 4a confirm that the stationary WDF classicality behavior emerges when the decoherence rises.

Conclusions

This study examines the WDF non-classicality dynamics of a system with a resonator coherent field interacting with a qubit. The considered system is under intrinsic decoherence. The coupling between the qubit and the cavity is a two-photon interaction. For an initial even coherent resonator state, the non-classical dynamics of the phase space WDF and its partial distributions have been explored for an initial even coherent resonator state. Based on the resonator entropy dynamics, the times of the maximally and partially mixed coherent-resonator states have been chosen. By raising the detuning and the intrinsic decoherence, the produced mixedness resonator entropy can be increased as well. Detuning, decoherence, and the qubit-resonator interaction all affect the phase space WDF non-classicality dynamics. Detuning and intrinsic decoherence can entirely diminish or eradicate the non-classicality. For the initial largest negative and positive values of the WDF, the ability of the qubit-resonator interaction to generate WDF non-classicality is examined. The partial Wigner distributions wit respect to the phase space real and imaginer components, the collapse and revival phenomena are reported. The qubit-resonator detuning leads to asymmetric WDF non-classicality behavior. While the appearance of stationary Wigner-distribution non-classicality is observed during the time-partial Wigner distribution dynamics. The WDF non-classicality can be further enhanced by the detuning.

CRediT authorship contribution statement

Laila A. Al-essa: Resources, Software, Writing – original draft. **Wafa F. Alfwzan:** Investigation, Methodology, Resources, Writing – original draft. **F.M. Aldosari:** Data curation, Investigation, Methodology, Writing – original draft. **A.-B.A. Mohamed:** Data curation, Investigation, Writing – original draft. **H. Eleuch:** Investigation, Supervision, Writing – review & editing.

Declaration of competing interest

The authors declare no conflicts of interest.

Data availability

No data was used for the research described in the article.

Acknowledgments

This work was funded by the Deanship of Scientific Research at Princess Nourah bint Abdulrahman University, through the Research Groups Program Grant no. (RGP-1444-0053). All authors typed, read, and approved the final manuscript.

References

[1] Wigner EP. Phys Rev 1932;47:749.
[2] Husimi K. Proc Phys Math Soc Japan 1940;22:264.
[3] Fakhri H, Sayyah-Fard M. Sci Rep 2021;11:22861.
[4] Thapliyal K, Banerjee S, Pathak A, Omkarc S, Ravishankar V. Ann Phys 2015;362:261.
[5] Banerji A, Singh RP, Bandyopadhyay A. Opt Commun 2014;330:85.
[6] Ghorbani M, Faghihi MJ, Safari H. J Opt Soc Amer B 2017;34:1893.
[7] Harder G, Silberhorn C, Rehacek J, Hradil Z, Motka L, Stoklasa B, et al. Phys Rev Lett 2016;116:133601.
[8] Ferrie Ch, Morris R, Emerson J. Phys Rev A 2010;82:044103.
[9] Mohamed A-B, Eleuch H. Eur Phys J D 2015;69:191.
[10] Siyouri F-Z, Mansour HA. Quantum Inf Process 2021;20:136.
[11] Hou L-L, Chen X-F, Wang S. Optik 2020;220:165013.
[12] Ra Y-S, Dufour A, Walschaers M, Jacquard C, Michel T, Fabre C, et al. Nat Phys 2020;16:144.
[13] Mohamed A-BA, Eleuch H. Sci Rep 2020;10:13240.
[14] Dehghani A, Mojaveri B, Aryaie M. Internat J Theoret Phys 2023;62:5.
[15] Dehghani A, Mojaveri B, Aryaie M. Quantum Inf Process 2022;21:45.
[16] Cochrane PT, Milburn GJ, Munro WJ. Phys Rev A 1999;59:2631.
[17] Zhang JQ, Xiong W, Zhang S, Li Y, Feng M. Ann Physics 2015;527:180.
[18] Mohamed A-BA, Hashem M, Eleuch H. Entropy 2019;21:672.
[19] van der Wal CH, ter Haar ACJ, Wilhelm FK, Schouten RN, Harmans CJPM, Orlando TP, et al. Science 2000;290:773.
[20] Brune M, Hagley E, Dreyer J, Maître X, Maali A, Wunderlich C, et al. Phys Rev Lett 1996;77:4887.
[21] Ourjoumtsev A, Jeong H, Tualle-Brouri R, Grangier P. Nature 2007;448:784.
[22] Stufler S, Machnikowski P, Ester P, Bichler M, Axt VM, Kuhn T, et al. Phys Rev B 2006;73:125304.
[23] Yuan HY, Zheng S, Ficek Z, He QY, Yung M-H. Phys Rev B 2020;101:014419.
[24] Mohamed A-BA, Eleuch H. Eur Phys J Plus 2022;137:853.
[25] Puebla R, Hwang M-J, Casanova J, Plenio MB. Phys Rev A 2017;95:063844.
[26] Yang WL, Yin ZQ, Xu ZY, Feng M, Oh CH. Phys Rev A 2011;84:043849.
[27] Abdel.Aty A-H, Kadry H, Mohamed A-BA, Eleuch H. Sci Rep 2020;10:16640.
[28] Buluta I, Ashhab S, Nori F. Rep Progr Phys 2011;74:104401.
[29] You JQ, Nori F. Phys Today 2005;58:42.
[30] Armenta Rico RJ, Maldonado-Villamizar FH, Rodriguez-Lara BM. Phys Rev A 2020;101:063825.
[31] Wallraff A, Schuster DI, Blais A, Frunzio L, Huang R-S, Majer J, et al. Nature 2004;431:162.
[32] Gu X, Kockum AF, Miranowicz A, Liu YX, Nori F. Phys Rep 2017;718:1.
[33] Huang R, Miranowicz A, Liao J-Q, Nori F, Jing H. Phys Rev Lett 2018;121:153601.
[34] Garziano L, Ridolfo A, Miranowicz A, Falci G, Savasta S, Nori Franco. Sci Rep 2020;10:21660.
[35] Wang X, Miranowicz A, Li H-R, Nori F. Phys Rev A 2017;96:063820.
[36] Burkard G, DiVincenzo DP, Bertet P, Chiorescu I, Mooij JE. Phys Rev B 2005;71:134504.
[37] Asadian A, Brukner C, Rabl P. Phys Rev Lett 2014;112:190402.
[38] Felicetti S, Rossatto DZ, Rico E, Solano E, Forn-Díaz P. Phys Rev A 2018;97:013851.
[39] Goeppert-Mayer M. Ann der Phys 1931;409:273.
[40] Taghipour J, Mojaveri B, Dehghani A. Eur Phys J 2022;137:772.
[41] Taghipour J, Mojaveri B, Dehghani A. Modern Phys Lett A 2022;37:2250141.
[42] Rohith M, Sudheesh C. Phys Rev A 2015;92:053828.
[43] Mohamed A-BA, Eleuch H. Eur Phys J Plus 2017;132:75.
[44] Milburn GJ. Phys Rev A 1991;44:5401.
[45] Kuang L-M, Tong Z-Y, Ouyang Z-W, Zeng H-S. Phys Rev A 1999;61:013608.
[46] Breuer H-P, Petruccione F. The theory of open quantum systems. Oxford University Press; 2002.
[47] Zhong W, Sun Z, Ma J, Wang X, Nori F. Phys Rev A 2013;87:022337.

[48] Wang X, Miranowicz A, Liu Y-X, Sun CP, Nori F. Phys Rev A 2010;81:022106.
[49] Eleuch H, Rotter I. Phys Rev A 2016;93:042116.
[50] Eleuch H, Rotter I. Eur Phys J D 2015;69:229.
[51] Wu Y-L, Deng D-L, Li X, Sarma SD. Phys Rev B 2017;95:014202.
[52] Stassi R, Cirio M, Nori F. npj Quantum Inf 2020;6:67.
[53] de Oliveira MC, Munro WJ. Phys Lett A 2004;320:352.
[54] Chao Shi-Lei, Xiong Biao, Zhou Ling. Ann Phys (Berlin) 2019;53:1900196.
[55] He ZH, Xiong ZH, Zhang YL. Phys Lett A 2006;354:79.
[56] Cahill KE, Glauber RJ. Phys Rev 1968;177:1882.
[57] Moya-Cessa Héctor, Peter LKnight. Phys Rev A 1993;48:2479.
[58] Hessian HA, Mohamed A-BA. Laser Phys 2008;18:1217.
[59] Araki H, Lieb E. Comm Math Phys 1970;18:160.
[60] Phoenix SJD, Knight PL. Phys Rev A 1991;44:6023.
[61] Bennett CH, Bernstein HJ, Popescu S, Schumacher B. Phys Rev A 1996;53:2046.
[62] Obada A-SF, Hessian HA, Mohamed A-BA. Opt Commun 2007;280:230.
[63] Zhang B. Opt Commun 2010;283:4676.
[64] Thapliyal K, Peřina J. Phys Lett A 2019;383:2011.